Beam-Halo Measurements in High-Current Proton Beams

C. K. Allen,[1] K. C. D. Chan,[1] P. L. Colestock,[1] K. R. Crandall,[2] R. W. Garnett,[1] J. D. Gilpatrick,[1] W. Lysenko,[1] J. Qiang,[3] J. D. Schneider,[1] M. E. Schulze,[4] R. L. Sheffield,[1] H. V. Smith,[1] and T. P. Wangler[1]

[1]*Los Alamos National Laboratory, Los Alamos, New Mexico 87544*
[2]*TechSource, Santa Fe, New Mexico 87594-1057*
[3]*Lawrence Berkeley National Laboratory, Berkeley, California 94720*
[4]*General Atomics, Los Alamos, New Mexico 87545*

(Received 25 July 2002; published 4 November 2002)

We present results from an experimental study of the beam halo in a high-current 6.7-MeV proton beam propagating through a 52-quadrupole periodic-focusing channel. The gradients of the first four quadrupoles were independently adjusted to match or mismatch the injected beam. Emittances and beamwidths were obtained from measured profiles for comparisons with maximum emittance-growth predictions of a free-energy model and maximum halo-amplitude predictions of a particle-core model. The experimental results support both models and the present theoretical picture of halo formation.

DOI: 10.1103/PhysRevLett.89.214802 PACS numbers: 29.17.+w, 29.27.Bd, 41.75.–i, 41.85.Ew

Beam halo is a major cause of beam loss and radioactivation in high beam-power proton linacs. Understanding the mechanisms of halo formation is important for a new generation of high-intensity linacs with future applications that include spallation-neutron sources, neutrino factories, and accelerator driven subcritical reactors for nuclear-waste transmutation. More than a decade ago, computer simulation studies [1] identified beam mismatch as the major source of the halo and emittance growth seen in simulations. The emittance growth can also be related to the conversion of beam free energy from mismatch oscillations into thermal energy of the beam. For a given mismatch strength, the free-energy model determines the maximum emittance growth resulting from the complete transfer of free energy into emittance [2].

A physical model of halo formation is expected to include both nonlinear and time-dependent forces to drive halo particles to larger amplitudes. Such a mechanism is provided by a particle-core model [3–5], in which beam mismatch produces an imbalance between focusing, space charge, and emittance, exciting a symmetric or breathing (x_{rms} and y_{rms} in phase) mode oscillation of the core. The space-charge field of the oscillating core modulates the net focusing force acting on individual particles and drives particles in a nonlinear parametric resonance when $f_{\mathrm{particle}} = f_{\mathrm{mode}}/2$, where f_{particle} is the betatron frequency of the particle and f_{mode} is the mode-oscillation frequency [4]. The model predicts a maximum resonant-particle amplitude as a function of the mismatch strength [5]. Neither model predicts the growth rates for the halo amplitude and beam emittance, for which numerical simulations are required.

To test the models, we installed a 52-quadrupole periodic-focusing beam-transport channel at the end of the Los Alamos low-energy demonstration accelerator (LEDA). LEDA delivers a 6.7-MeV proton beam from a 350-MHz radio frequency-quadrupole (RFQ) linac. For these measurements [6–9] the beam was pulsed at a 1-Hz rate with a 30-μs pulse length. The channel length of 11 m was sufficient for the development of about ten mismatch oscillations, enough to observe at least the initial stages of emittance growth and halo formation caused by mismatch. In this paper we present results for a 75-mA beam current. Data acquired at three other beam currents will be reported later.

The most important diagnostic elements were the transverse beam-profile scanners [10], each of which contains two distinct components. First is a 33-μm-diameter carbon wire from which secondary electrons are released when the wire intercepts the proton beam, allowing a beam-profile measurement of the dense beam core. Second is a pair of 1.5-mm-thick graphite scraper plates, thick enough to stop the protons, for measurement of the outer beam profiles. The magnitudes of the charge detected from the wires and the plates are combined in the software to produce a single beam-profile distribution. Scanners at nine stations (Fig. 1), each located midway between pairs of quadrupoles, measured the horizontal and vertical distributions. The scanners were labeled with numbers corresponding to the preceding quadrupole-magnet number.

The beam was matched, using a least-squares fitting procedure that adjusted the first four quadrupoles to produce equal rms sizes at the last eight scanner locations. The program TRACE3D [11] was used to calculate

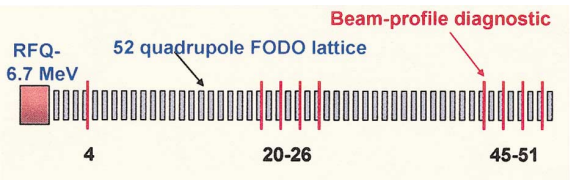

FIG. 1 (color). Block diagram of the 52-quadrupole-magnet lattice showing the nine locations of beam-profile scanners.

the Courant-Snyder phase-space ellipse parameters of the matched beam. For a mismatched beam one must consider not only the breathing mode, but also the antisymmetric or quadrupole mode. The pure eigenmode mismatch settings of the four matching quadrupoles were calculated by appropriate scaling of the matched Courant-Snyder parameters [12]. The mismatch strength was measured by a mismatch parameter μ, which equals the ratio of the rms size of the initial beam to that of the matched beam. For a matched beam $\mu = 1$.

Figure 2 shows the matched and mismatched 75-mA beam profiles at scanner 51. The matched beam has a Gaussian-like central profile with a rms-beam size of 1.1 mm. For the matched beam a low-density halo is observed to extend as far as 9 rms. This matched-beam halo is observed at all scanners and is most easily explained as a halo that has formed in the injector/RFQ system prior to the periodic quadrupole channel. Direct measurement of the beam-energy distribution with a resolution of about 200 keV, using a dispersive section of the transport line at the end of the periodic quadrupole channel, shows no evidence for low-energy tails that might contribute to this halo. Although collimation can remove this halo, collimation was not implemented in our experiment. Halo caused by mismatch was our main interest, because this mismatch mechanism is expected to involve more particles and can form halo even at high energy where collimation is more difficult. A breathing-mode-mismatch beam profile for $\mu = 1.5$, seen in Fig. 2, shows the growth of shoulders indicating substantial formation of halo.

The rms-size measurements were used to calculate the rms emittances at scanners 20 and 45. The scanner 20 emittances were obtained from the rms-beam sizes at scanners 20, 22, 24, and 26, and the scanner 45 emittances were obtained from scanners 45, 47, 49, and 51. For each case the rms emittances were obtained from a least-squares fit in which the squared differences between measured and calculated (using TRACE3D to trace the beam envelopes) rms-beam sizes were minimized by adjusting the emittances and Courant-Snyder parameters. After the emittances were obtained from the fitted data, tune depressions (ratio of betatron phase advance per focusing period with space charge to without space charge) were calculated from TRACE3D. For the matched beam at 75 mA, the measured unnormalized rms emittances at scanner 20 were $\varepsilon_x = 3.0 \pm 0.2$ mm mrad, and $\varepsilon_y = 3.1 \pm 0.2$ mm mrad. Assuming zero emittance growth in the channel for the matched beam, the tune depression from space charge was 0.82 immediately after the matching quadrupoles at scanner 4, and was constant at 0.95 after the beam had debunched at approximately quadrupole 16, about 3.5 m from the beginning of the channel. Although the beam was not in a space-charge-dominated regime, significant space-charge effects in mismatched beams were still expected.

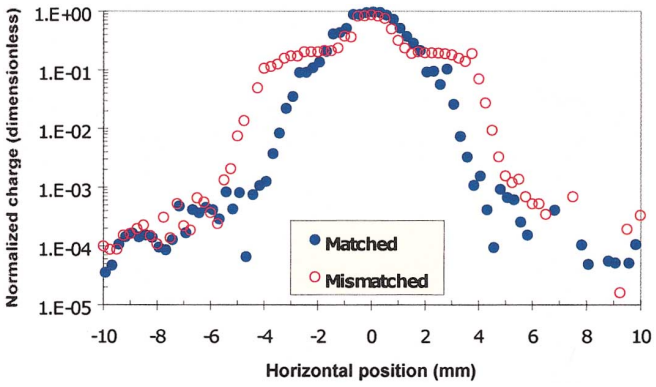

FIG. 2 (color). Horizontal beam profiles at scanner 51 for a 75-mA, $\mu = 1$ matched beam (blue solid circles), and breathing-mode $\mu = 1.5$ mismatched beam (red open circles).

The free-energy model can be tested by comparing the measured emittance growths at scanners 20 and 45 with the emittance-growth upper limits from that model. The emittance-growth measurements for mismatched beams show some significant anisotropies (x-y differences). Franchetti, Hofmann, and Jeon [13] report simulation studies of anisotropic beams in uniform focusing channels, in which large (40%) x-y emittance-growth differences are observed that are sensitive to initial x-y tune differences as small as 1%. The sensitivity is not the result of chaotic behavior, but is caused by the parametric resonance discussed earlier, which is sensitive to x-y parameter differences. In our case, anisotropies could be driven by percent-level input x-y emittance differences that are not resolved experimentally. Although the free-energy model was derived for an axisymmetric beam, these authors find that the model can be extended to a 2D anisotropic case if the emittance growth is averaged over x and y.

Figure 3 shows the x-y averaged rms-emittance-growth results (points with error bars) versus μ at scanner 20 for a 75-mA breathing-mode mismatch. The maximum emittance-growth curves from the free-energy model are shown for the two tune-depression values that bracket the values for the debunching beam, and it can be seen that the theoretical maximum is insensitive to the tune depression over this range. The breathing-mode data in Fig. 3 are consistent at all μ values with the maximum emittance growth predicted by the model. The breathing-mode results at scanner 45 (not shown) show no significant additional emittance growth, consistent with the upper limits from the model and with complete transfer of free energy within only four mismatch oscillations. Quadrupole mismatch data at 75 mA are not available at scanner 20, but are available at scanner 45 (see Fig. 4). These results are also consistent at all measured μ values with the maximum growth of the model. Although an axisymmetric beam is assumed in the model, applicability to the quadruple mode is physically reasonable for

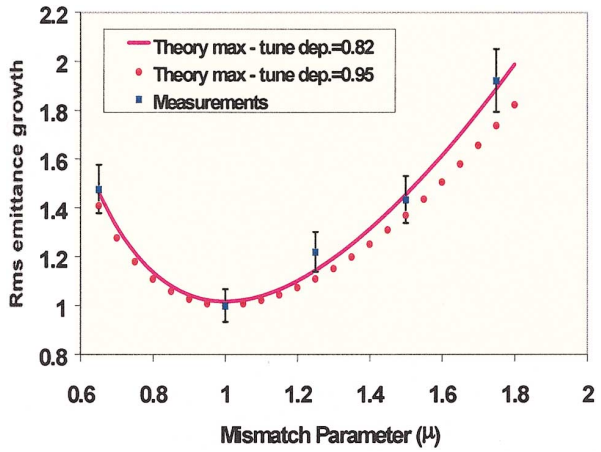

FIG. 3 (color). Measured rms-emittance growth averaged over x and y for 75 mA at scanner 20 for a breathing-mode mismatch. The curves show maximum growth from the free-energy model.

a given free energy if equal energy sharing is assumed in x and y. Overall, the data for both mismatch modes indicate a rapid growth mechanism with nearly complete transfer of free energy occurring in less than ten mismatch oscillations.

The particle-core model predicts the maximum resonant-particle amplitude as a function of mismatch parameter μ [5]. We were unable to determine an experimental maximum amplitude for direct comparison because of background. Instead, we compare the measured amplitudes (x-y averaged half-widths of the beam) at three different fractional beam-profile intensity levels (10%, 1%, and 0.1% of the peak) for a breathing-mode mismatch with the maximum amplitude predicted by the particle-core model. A comparison is shown in Fig. 5 for scanner 20 at 75 mA. The shapes of all three measured half-width curves are consistent with the shape of the maximum amplitude curve from the particle-core model, and all three measured curves lie below the maximum amplitude curve from the model. Similar results are observed at scanner 51.

Although the particle-core model based on a single mismatch mode is a simple description of the beam dynamics, the agreement with the model for the curve shapes and for the consistency of the magnitudes supports the conclusion that the model incorporates the main physical mechanism responsible for the halo growth. When applying the model, it may be wise to allow a margin in the range of ~20% to anticipate a larger amplitude in one plane from unavoidable errors that could lead to x-y anisotropy.

The 6D-density distribution at the input to the transport channel, needed for multiparticle simulations, is not experimentally known. We find that knowledge of the input Courant-Snyder parameters and emittances alone is not sufficient for reliable multiparticle simulations of the halo. Breathing-mode, 75-mA simulations beginning with three different input distributions (6D Waterbag, 6D Gaussian, and a distribution obtained from a simulation from the ion source through the RFQ called LEBT/RFQ) all underestimate the halo growth rate (see Table I) [14]. Input distributions with greater population in the tails produce larger emittance-growth rates, as is shown in Ref. [14] using a double-Gaussian input distribution. This trend is consistent qualitatively with the particle-core model, since the resonance condition is satisfied only for particles outside the core. Agreement between simulations and experiment for the growth rate requires an input distribution that represents more accurately the tails of the real input beam.

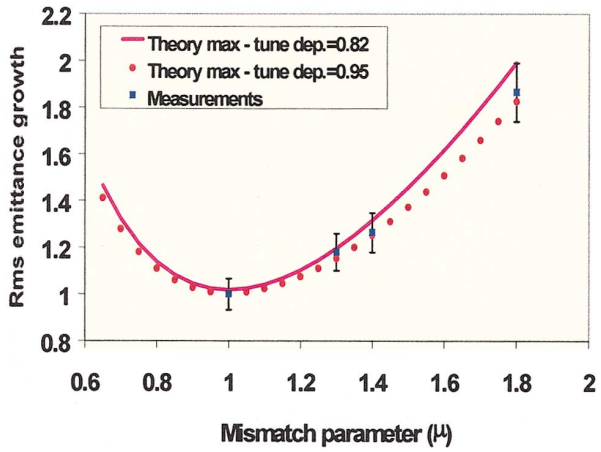

FIG. 4 (color). Measured rms-emittance growth averaged over x and y for 75 mA at scanner 45 for a quadrupole-mode mismatch. The curves show maximum growth from the free-energy model.

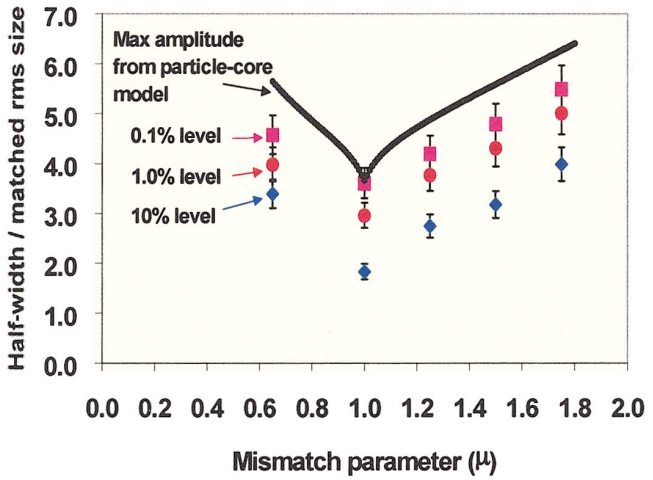

FIG. 5 (color). Measured beam half-widths at scanner 20 (75 mA and a breathing-mode mismatch) at different fractional intensity levels versus mismatch strength μ for comparison with the maximum resonant amplitude of the particle-core model. Equation (6) of Ref. [5] gives an approximate expression for the theory.

TABLE I. Emittance growth at scanner 45 from three simulations and from the experiment for a breathing mode, $\mu = 1.5$ and 75 mA.

Input distribution	Growth
6D Waterbag (simulation)	1.08
6D Gaussian (simulation)	1.18
LEBT/RFQ (simulation)	1.35
Experiment	1.51

In summary, our experimental results strongly support both models and the present theoretical picture of halo formation in mismatched beams. This result is important because these models predict upper limits to emittance and halo-amplitude growth in high-current transport channels and linacs and allow estimation of focusing strength and aperture requirements in new designs.

We thank the dedicated LEDA personnel who made the experiment possible. We thank Ingo Hofmann for sending a draft of their paper on anisotropy effects in mismatched beams, which helped us to interpret our results. We thank Lloyd Young for providing a multiparticle simulation used to generate one of our input beams. We thank Martin Reiser, Ingo Hofmann, Jerry Nolen, Pat O'Shea, and Irving Haber for helpful conversations. This work was supported by the U.S. Department of Energy. Simulations in this research were performed in part using resources of the National Energy Research Scientific Computing Center, which is supported by the Office of Science of the U.S. Department of Energy.

[1] A. Cucchetti *et al.*, in *Proceedings of the IEEE 1991 Particle Accelerator Conference*, edited by L. Lizama and J. Chew (IEEE, New York, 1991), p. 251.
[2] M. Reiser, *Theory and Design of Charged Particle Beams* (Wiley, New York, 1994), pp. 470–473; M. Reiser, J. Appl. Phys. **70**, 1919 (1991).
[3] J. S. O'Connell, T. P. Wangler, R. S. Mills, and K. R. Crandall, in *Proceedings of the 1993 Particle Accelerator Conference* (IEEE Catalog No. CH3279-7), pp. 3657–3659.
[4] R. L. Gluckstern, Phys. Rev. Lett. **73**, 1247 (1994).
[5] T. P. Wangler, K. R. Crandall, R. Ryne, and T. S. Wang, Phys. Rev. ST Accel. Beams **1**, 084201 (1998).
[6] P. L. Colestock *et al.*, in *Proceedings of the 2001 Particle Accelerator Conference* (IEEE Catalog. No. 01CH37268), pp. 170–172.
[7] M. Schulze *et al.*, in *Proceedings of the 2001 Particle Accelerator Conference* (Ref. [6]), pp. 591–593.
[8] T. P. Wangler *et al.*, in *Proceedings of the 2001 Particle Accelerator Conference* (Ref. [6]), pp. 2923–2925.
[9] T. P. Wangler, in *Proceedings of the 20th ICFA Workshop, Fermilab, 2002* (American Institute of Physics, New York, 2002).
[10] J. D. Gilpatrick *et al.*, in *Proceedings of the 2001 Particle Accelerator Conference* (Ref. [6]), pp. 525–527.
[11] K. R. Crandall and D. P. Rusthoi, Los Alamos Report No. LA-UR-97-886, 1997.
[12] T. P. Wangler, Los Alamos Report No. LA-UR-00-3181, 2000.
[13] G. Franchetti, I. Hofmann, and D. Jeon, Phys. Rev. Lett. (to be published).
[14] Ji Qiang *et al.*, Phys. Rev. ST Accel. Beams (to be published).